Int J Clin Exp Med 2018;11(8):7740-7750
www.ijcem.com /ISSN:1940-5901/IJCEM0070283

Original Article

Identification of key genes and pathways in human glioblastoma multiforme by co-expression analysis

Lei Shi[1*], Yongwen Luo[2*], Jianxiang Wang[1], Chengan Cao[1], Xiang Peng[1]

Departments of [1]Neurosurgery, [2]Urology, Pu'ai Hospital, Tongji Medical College, Huazhong University of Science and Technology, Wuhan, China. [*]Equal contributors.

Received December 3, 2017; Accepted May 14, 2018; Epub August 15, 2018; Published August 30, 2018

Abstract: Glioblastoma multiforme (GBM) is one of the most common malignant primary brain tumors in adults. Its prognosis is influenced by progression covering a complex network of gene interactions. In this study, microarray expression data of GBM (n = 114) and normal brains (n = 17) were analyzed to identify 3,523 differently expressed genes (DEGs), in which protein-protein interaction (PPI) and weighted gene co-expression networks were constructed to identify key genes and pathways associated with occurrence and progression of GBM. The top 6 hub genes (*CACNA1C, TOP2A, CDK1, DLG4, EGFR,* and *CDC42*) with the highest connectivity degree in the PPI network were identified and then validated. In the weighted gene co-expression network, 9 GBM-related modules were identified. Of which, 7 were found to be stable after performing module preservation analysis. Genes in the 7 modules were associated with cell division and differentiation, cell proliferation, cell adhesion, immune response, metabolic process, cell cycle regulation, neuron development, and transmembrane transport. This study illustrates that hub genes and pathways are involved in the progression of GBM. Further molecular biological experiments are necessary to confirm the function of candidate biomarkers in human GBM.

Keywords: Glioblastoma multiforme (GBM), differentially expressed genes (DEGs), biomarker, weighted gene co-expression network analysis (WGCNA), protein-protein interaction (PPI)

Introduction

Glioblastoma multiforme (GBM) is one of the most common malignant primary brain tumors in adults [1]. Current treatment for GBM is, mainly, surgical resection combined with radiotherapy and chemotherapy [2]. The median survival time of high grade GBM is only 12-15 months [3]. At present, histological analysis of GBM tissue obtained by surgery is a necessary process for definitive diagnosis [4]. Therefore, screening GBM molecular markers will provide important clinical value for diagnosis, especially in cases of uncertain histological results or surgical contraindications.

Currently, gene expression profiles are used to identify genes associated with progression of GBM [5]. Additionally, some researchers have also used an integrated approach to screen changes in brain carcinogenesis [6]. However, most studies have focused on screening of differentially expressed genes and ignored the high degree of interconnection between genes, although genes with similar expression patterns may be functionally related. Weighted gene co-expression network analysis (WGCNA) has been used to construct a co-expression network based on relationship between genes and identifying significant gene modules and hub genes associated with tumor progression by constructing scale free gene co-expression networks [7]. At present, many studies perform WGCNA to screen key genes, modules, and pathways related with clinical characteristics such as tumor stage, grade, and metastasis among different tumor types, including papillary renal cell carcinoma [8] and hepatocellular carcinoma [9]. Thus, this study attempted to screen differentially expressed genes, then construct protein-protein interaction networks and a co-expression network of relationships between genes through a systematic biology method based on a weighted genome expression network (WGCNA), identifying key genes and pathways participating in progression of GBM.

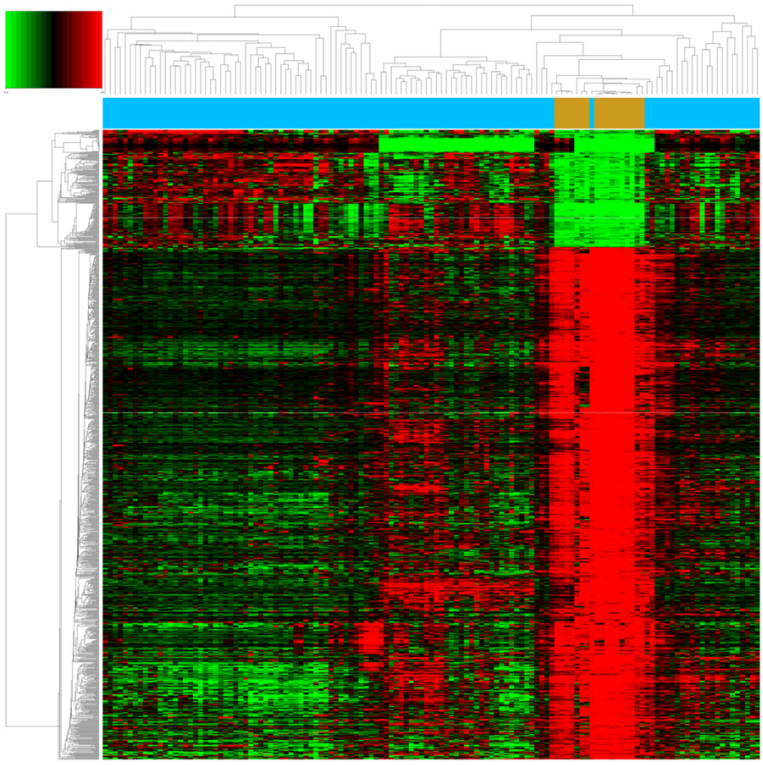

Figure 1. Heatmap of differentially expressed genes between 17 normal brain samples and 114 GBM samples. Red represents upregulated genes and green represents downregulated genes.

Materials and methods

Data collection

Gene expression profile was d*ownloaded from Gene Expression Omnibus (GEO) database* (http://www.ncbi.nlm.nih.gov/geo/). Dataset GSE7696 [10] and GSE50161 [11], both performed on Affymetrix Human Genome U133 Plus 2.0 Array (Affymetrix, Santa Clara, CA, USA), were combined and analyzed to screen differentially expressed genes and construct protein-protein interaction networks. Dataset GSE7696, including 80 GBM tissues and 4 normal brain tissues, was used to construct weighted gene co-expression networks and identify hub genes and pathways for this study. Another independent dataset GSE53733 [12], consisting 70 GBM tissues, was used for module preservation analysis.

Data preprocessing and differentially expressed genes (DEGs) screening

Raw expression data were calculated according to the pre-processing procedures: RMA background correction, log2 transformation, quantile normalization, and median polish algorithm summarization using the "affy" [13] R package. Besides, "va" [14] R package was used to remove batch effects between dataset GSE7696 and GSE50161. Probes were annotated by the Affymetrix annotation files. "limma" [15] R package was used to screen the DEGs between 114 GBM samples and 17 normal brain samples. Cut-off criteria for screening DEGs were FDR (false discovery rate) < 0.01 and |log2fold change| ≥ 1.

PPI network construction and hub cluster detection

Search Tool for Retrieval of Interacting Genes (STRING) Database (http://www.string-db.org/) [16] was used to construct protein-protein interaction (PPI) networks. Confidence scores > 0.7 were set as significant. In the PPI network, genes with connectivity degree of ≥ 60 were also defined as hub genes. Cytoscape software [17] was used for network visualization. Plug-in Molecular Complex Detection (MCODE) [18] in Cytoscape was used to identify hub cluster from PPI network. Cut-off criteria were degree = 2, node score = 0.2, k-core = 2, and max. depth = 100. Genes in hub clusters were uploaded to DAVID database [19] to conduct GO functional enrichment analysis.

Co-expression network construction and module preservation analysis

Scale-free gene co-expression networks were constructed by "WGCNA" R package. Briefly, expression data profiles of DEGs were tested to check if they were good samples and good genes. Pearson's correlation matrices were performed for all pair-wise genes. A weighted adjacency matrix was then constructed using a power function amn = |cmn|β (cmn = Pearson's correlation between gene m and gene n; amn = adjacency between gene m and gene n). β was

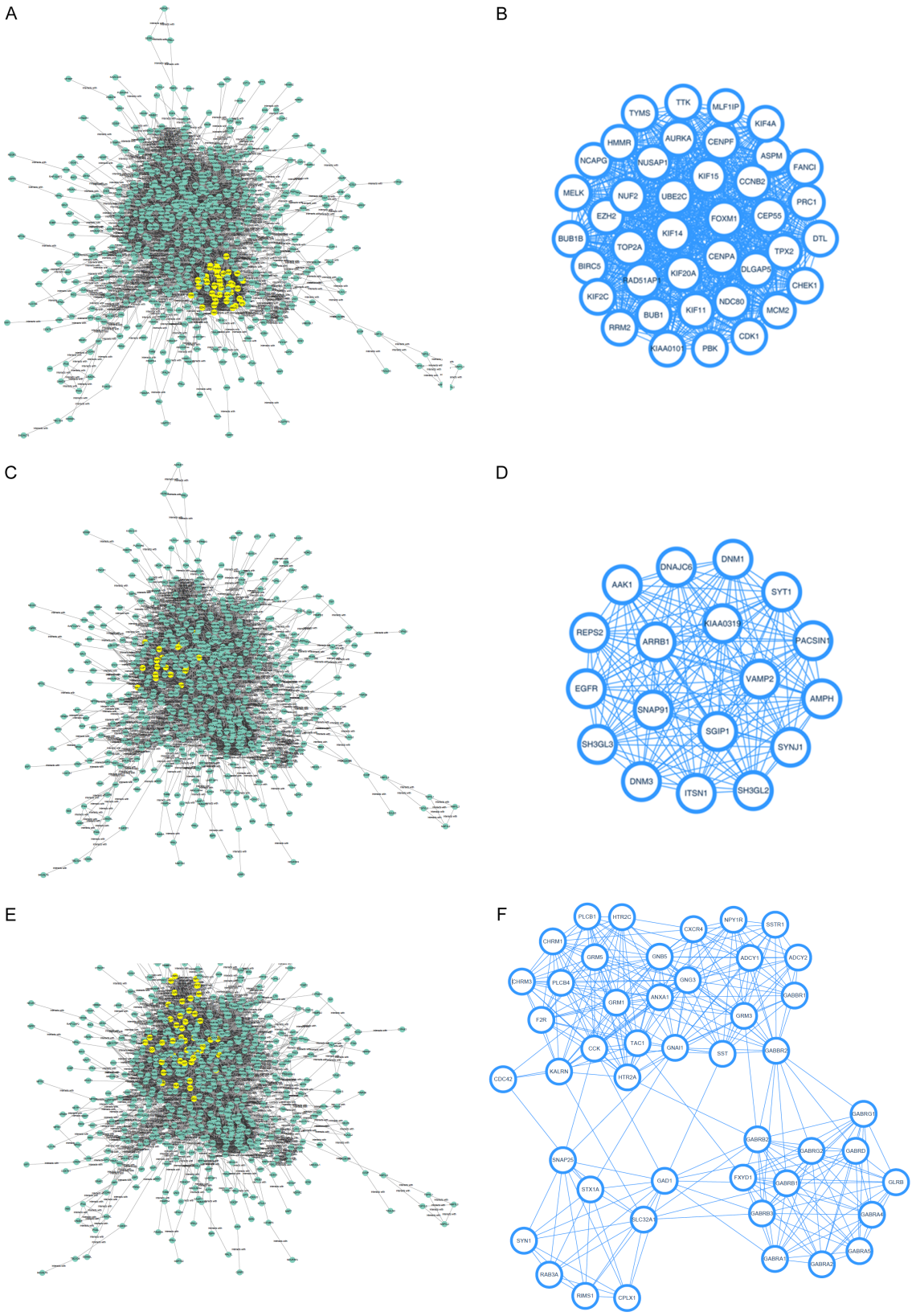

Figure 2. Hub cluster detection in PPI network. A. Cluster rank 1 in the whole PPI network. B. Cluster rank 1. C. Cluster 2 in the whole PPI network. D. Cluster rank 2. E. Cluster rank 3 in the whole PPI network. F. Cluster rank 3.

Table 1. GO enrichment analysis of the 3 clusters in PPI network

Cluster	GO ID	GO term	*P* value	Genes
Cluster 1	0007018	Microtubule-based movement	6.81E-07	KIF14, KIF2C, KIF4A, KIF11, KIF15, KIF20A
Cluster 1	0000910	Cytokinesis	0.0019	PRC1, BIRC5, KIF20A
Cluster 1	0090307	Mitotic spindle assembly	0.0021	KIF11, TPX2, BIRC5
Cluster 1	0000086	G2/M transition of mitotic cell cycle	0.0023	FOXM1, CHEK1, BIRC5
Cluster 1	0046602	Regulation of mitotic centrosome separation	0.0109	KIF11, CHEK1
Cluster 2	2000369	Regulation of clathrin-mediated endocytosis	0.0038	AAK1, DNAJC6
Cluster 2	0048268	Clathrin coat assembly	0.0102	SNAP91
Cluster 2	0097320	Membrane tubulation	0.0102	PACSIN1, SGIP1
Cluster 3	0007214	Gamma-aminobutyric acid signaling pathway	1.26E-18	GABRG1, GABRG2, GABRA2, GABRA1, GABRA4, GABRA5, GABBR1, GABBR2
Cluster 3	1902476	Chloride transmembrane transport	4.29E-12	FXYD1, GABRG2, GLRB, GABRA2, GABRA1, GABRA4, GABRB2, GABRB1, GABRA5
Cluster 3	0071420	Cellular response to histamine	1.04E-06	GABRG2, GABRB3, GABRB2, GABRB1
Cluster 3	0051966	Regulation of synaptic transmission, glutamatergic	1.64E-05	GRM5, GRM3, GRM1, KALRN
Cluster 3	0060119	Inner ear receptor cell development	1.47E-04	GABRB3, GABRB2, GABRA5

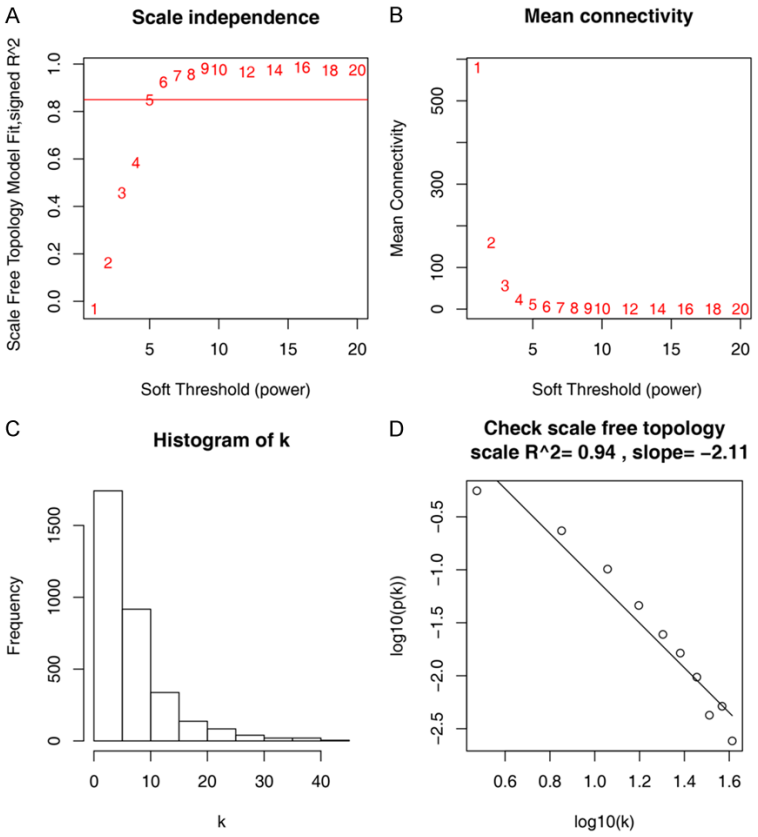

Figure 3. Determination of soft-thresholding power in weighted gene co-expression network analysis (WGCNA). A. Analysis of the scale-free fit index for various soft-thresholding powers (β). B. Analysis of the mean connectivity for various soft-thresholding powers. C. Histogram of connectivity distribution when β = 6. D. Checking the scale free topology when β = 6.

a soft-thresholding parameter that could emphasize strong correlation between genes and penalize weak correlation. Next, adjacency was transformed into topological overlap matrix (TOM), which could measure network connectivity of a gene defined as the sum of its adjacency with all other genes for network generation. To classify genes with similar expression profiles into gene modules, average linkage hierarchical clustering was conducted according to TOM-based dissimilarity measurement, with a minimum size (gene group) of 30 for the genes dendrogram. To further analyze the module, the dissimilarity of module eigengenes was calculated. Researchers chose a cut line (0.25) for module dendrogram and merged some modules. To access the stability of each identified module, module preservation and quality statistics were computed with the modulePreservation [20] function (nPermutations = 100) implemented by the WGCNA package.

Functional and pathway enrichment analysis of each module

Database for Annotation, Visualization, and Integrated Discovery (DAVID) [19] (*http://david.abcc.ncifcrf.gov/*) online tool was used for

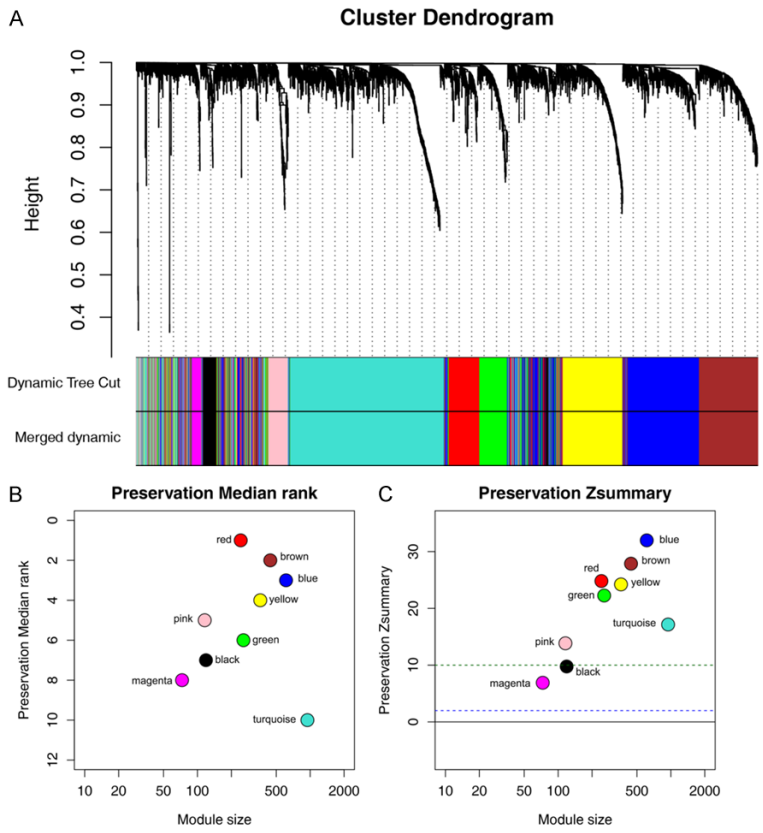

Figure 4. Clustering dendrograms of genes and module preservation analysis. (A) Gene clustering dendrogram generated by hierarchical clustering of adjacency-based dissimilarity. The colored row below the dendrogram indicates module membership identified by the dynamic tree cut method, together with assigned merged module colors and the original module colors. (B, C) MedianRank (B) and Zsummary (C) statistics of the module preservation of the 9 modules. In the left graph, medianRank of the modules close to zero indicates a high degree of module preservation. In the right graph, the dashed blue and green lines indicate the thresholds Z = 2 and Z = 10, respectively. These horizontal lines indicate Z summary thresholds for strong evidence of conservation (above 10) and for low to moderate evidence of conservation (above 2).

functional and pathway enrichment analysis. P < 0.05 was set as cut-off criterion.

Hub genes validation

Hub genes identified from PPI networks were validated by TCGA GBM RNA-seq data using Gene Expression Profiling Interactive Analysis (GEPIA, http://http://gepia.cancer-pku.cn/) [21].

Statistical analyses

Two-tailed Student's t-test was used for significance of differences between subgroups. Statistical analyses were performed with SPSS 16.0. Statistical significance was set at probability values of $P < 0.05$.

Results

Identification of DEGs in GBM tissues

GSE7696 and GSE50161, including 114 GBM samples and 17 normal brain samples, were analyzed. In total, 3,523 DEGs were identified using "limma" package of R software under the cut-off criteria of FDR < 0.01 and |log2fold change (FC)| ≥ 1, of which 1,192 were upregulated and 2,331 were downregulated. Heatmap of the DEGs is shown in **Figure 1**.

PPI network construction

A total of 3,523 DEGs were uploaded to STRING database. The PPI networks were constructed and visualized using Cytoscape software. Genes with higher connectivity degrees within a network play more important roles in biological processes [9]. Using the cut-off criteria of connectivity degree ≥ 60, the top 6 nodes with highest connectivity degrees were considered as hub nodes. These included CACNA1C, TOP2A, CDK1, DLG4, EGFR, and CDC42.

Hub cluster selection and functional annotation

With degree cut-off = 2, node score cut-off = 0.2, k-core = 2, and max. depth = 100 as the criterion, the top 3 significant clusters were identified using plug-in MCODE. Gene ontology (GO) analysis of each cluster was then performed in DAVID database (**Figure 2** and **Table 1**).

Weighted co-expression network construction and module preservation analysis

WGCNA was conducted on 3,523 DEGs of 80 GBM samples (GSE7696). "WGCNA" package was used in R, after quality assessment for

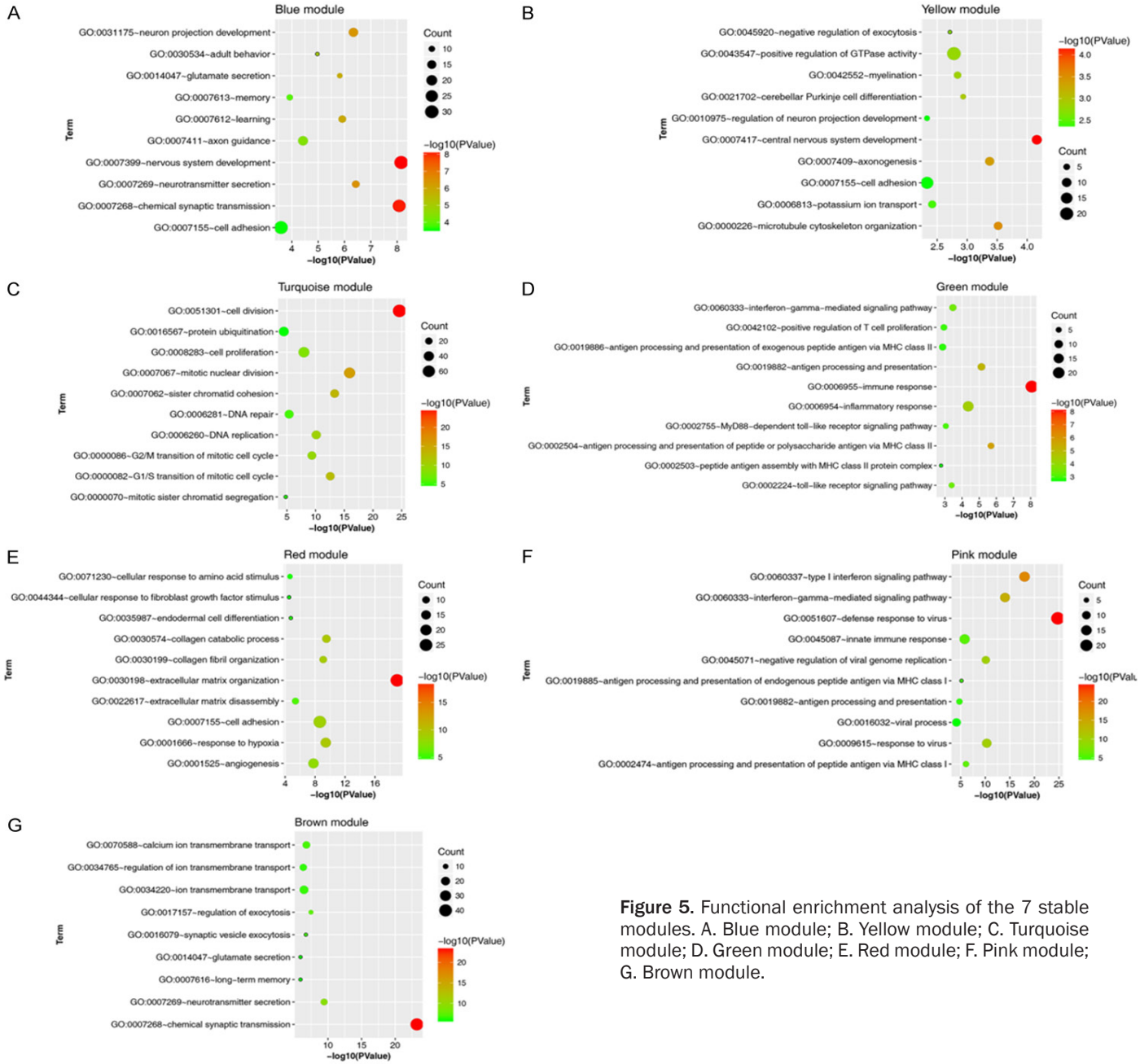

Figure 5. Functional enrichment analysis of the 7 stable modules. A. Blue module; B. Yellow module; C. Turquoise module; D. Green module; E. Red module; F. Pink module; G. Brown module.

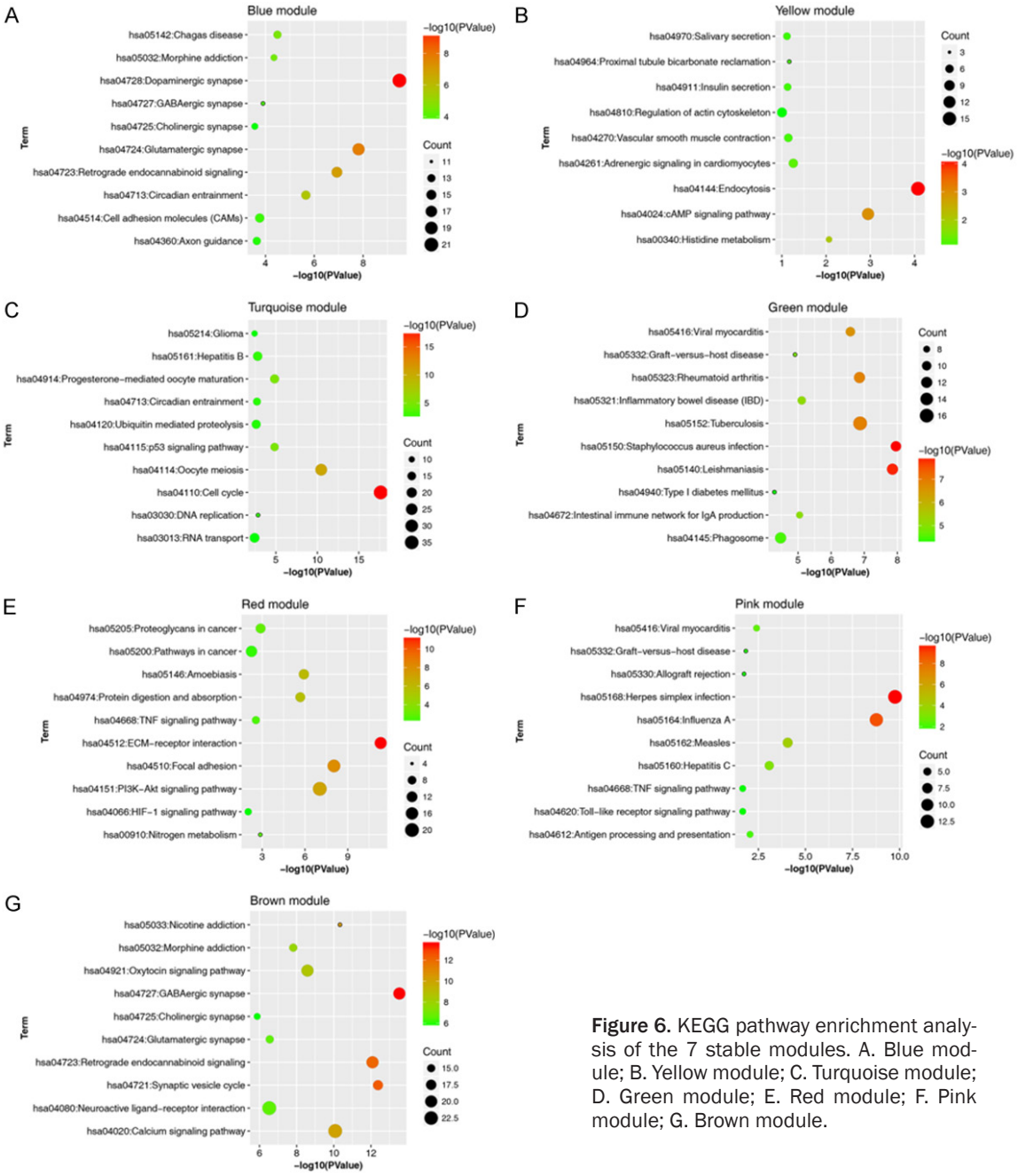

Figure 6. KEGG pathway enrichment analysis of the 7 stable modules. A. Blue module; B. Yellow module; C. Turquoise module; D. Green module; E. Red module; F. Pink module; G. Brown module.

expression data matrix of GSE53000, power of $\beta = 6$ (scale free $R^2 = 0.94$) was selected to ensure a scale-free network (**Figure 3A-D**). A total of 9 modules were identified after using average linkage clustering (**Figure 4A**). The "grey" module was reserved for genes identified as not co-expressed.

To determine whether identified networks could also be found in another independent network, summary preservation analysis was performed by comparing the GSE7696 data set with test data set GSE53733. Two modules, including "black" and "magenta", were found to be not stable and were excluded for subsequent analysis. The 7 remaining modules were stable enough, with Z summary statistics above 10 (**Figure 4B**, **4C**), to be selected for subsequent analysis.

Functional annotation and KEGG pathway enrichment of stable modules

Gene Ontology analysis was performed for the above 7 modules to explore underlying biologi-

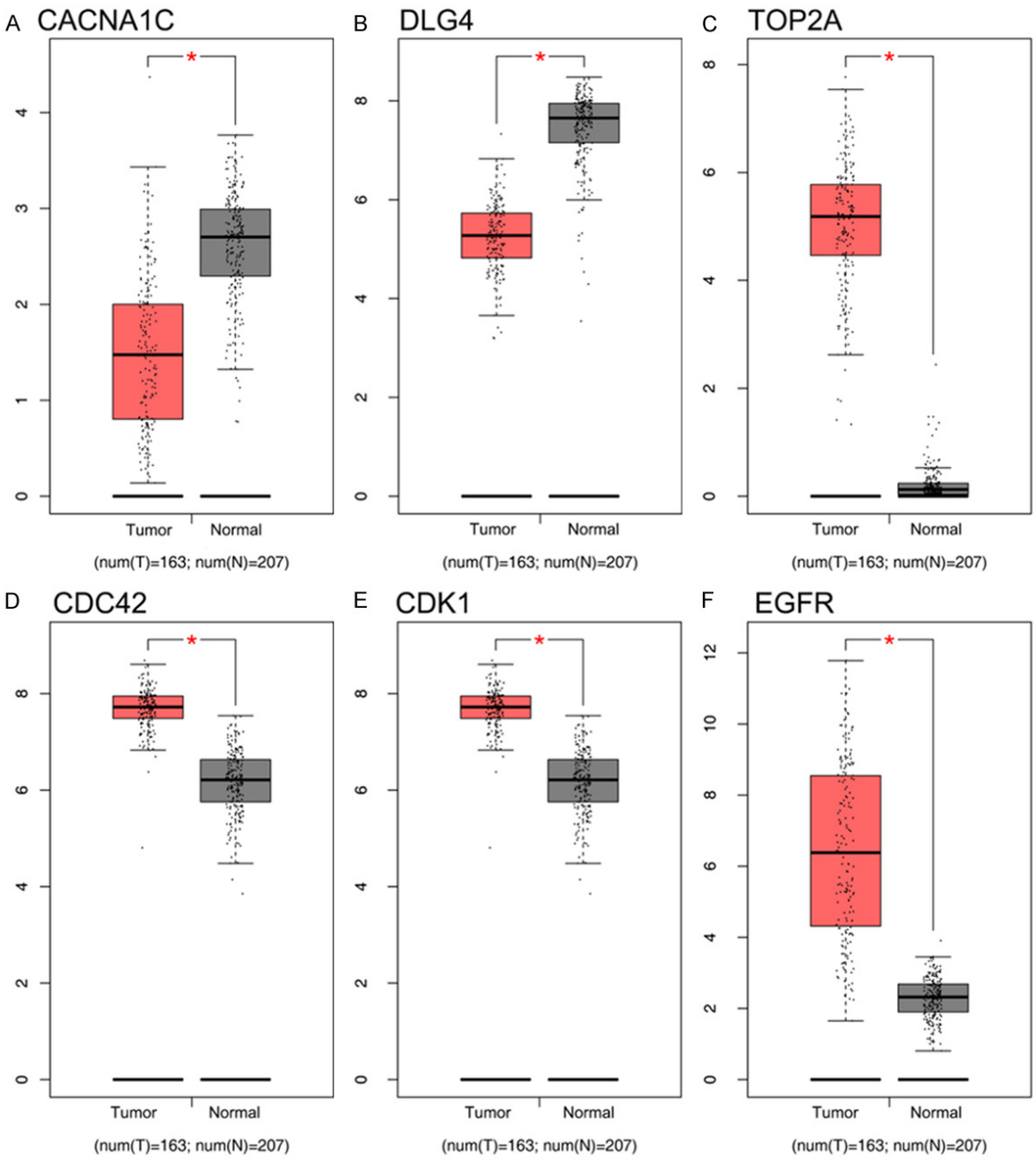

Figure 7. Validation of hub gene using TCGA GBM RNA-seq data.

cal processes correlated with GBM. As shown in **Figures 5** and **6**, genes in blue and yellow modules were significantly enriched in nervous system development and synaptic transmission. Genes in the turquoise module were mainly associated with cell division, cell proliferation, and cell cycle. Genes in green and pink modules were correlated with immune response and inflammatory response. Genes in the red module were mainly associated with extracellular matrix organization and cell division, which includes several significantly enriched pathways including EMC-receptor interaction, focal adhesion, and PI3K-Akt pathways. In the brown module, genes were enriched in ion transmembrane transport and exocytosis. Taken together, genes in the red modules were found to be most significantly correlated with GBM occurrence and progression.

Hub genes validation

Six hub genes were validated using TCGA GBM data. CACNA1C and DLG4 were significantly downregulated, in both microarray and TCGA GBM data, while the remaining 4 hub genes, including TOP2A, CDK1, EGFR, and CDC42, were significantly upregulated. This was consistent with the microarray data (**Figure 7**).

Discussion

Glioblastoma multiforme (GBM) is one of the most common malignant primary brain tumors in adults [1]. Currently, there are no specific molecular biomarkers for diagnosis and treatment of GBM. Therefore, it is essential to discover the molecular mechanisms of GBM [22]. In this study, gene expression profiles were examined, including 114 GBM samples and 17 normal brain samples, using integrated analysis to explore key genes and key pathway signaling playing key roles in GBM progression, possibly providing insight into diagnostic and therapeutic targets for GBM.

A total of 3,523 DEGs, including 1,192 upregulated and 2,331 downregulated, were screened from 114 GBM samples and 17 normal brain samples. PPI network analysis and WGCNA analysis were constructed to identify protein-protein interactions and gene co-expression modules. The 3 most significant gene clusters were identified from the PPI network, perhaps playing the most important role in the whole PPI network. Functional enrichment analysis was then performed, respectively, using genes in the 3 clusters. This analysis revealed that cell cycle regulation, mitotic regulation, and immune response might be significantly associated with progression of GBM. In addition, genes with higher connectivity degrees in a network play more important roles in biological processes [23]. Using cut-off criteria of ≥ 60, the top hub 6 nodes with highest connectivity degrees were identified. These included CACNA1C, TOP2A, CDK1, DLG4, EGFR, and CDC42. The 6 hub genes were validated by TCGA RNA-seq data of GBM. *TOP2A, CDC42,* and *CDK1* play important roles in regulation of cell cycle. They might exert key roles in GBM progression through regulating tumor cell cycle [24-26]. TOP2A has been reported to be a sensitive and specific biomarker indicating active cell proliferation [27]. In the current study, TOP2A was found to be a hub protein/gene in the PPI network, indicating a crucial role in regulating GBM progression, consistent with previous studies [27]. It has been observed that nearly 40% of GBM tumors demonstrate *EGFR* amplification, mostly associated with GBM recurrence and progression [28]. In this present study, *EGFR* was found to be a hub node in the PPI network, with subsequent validation demonstrating that it was significantly upregulated in GBM samples, also consistent with previous reports [29, 30]. CDK1 encodes CDKs, which function as a serine/threonine kinase and play an important role in cell cycle regulation [31]. Previous studies have reported that CDK1 promotes oncogenesis and progression of human gliomas, whereas downregulated CDK1 inhibits proliferation activities of human malignant gliomas [32]. Moreover, using plug-in MCODE in Cytoscape software, the 3 top clusters were identified. As shown in **Figure 2** and **Table 1**, genes in the 3 clusters were mainly associated with cell cycle regulation, cell division, and immune response, highlighting their key roles in regulating GBM progression.

Subsequently, WGCNA analysis identified 9 modules with a highly relevant expression pattern. Module preservation analysis demonstrated that 7 modules were stable in the test data set. Gene Ontology enrichment analysis was then performed to explore biological processes of the 7 modules. Genes within the same module exhibited a similar biological function. Genes in blue and yellow modules were significantly enriched in nervous system development and synaptic transmission. Genes in the turquoise module were mainly associated with cell division, cell proliferation, and cell cycle. Genes in green and pink modules were correlated with immune response and inflammatory response. Genes in the red module were mainly associated with extracellular matrix organization and cell division, with several significantly enriched pathways including EMC-receptor interaction, focal adhesion, and PI3K-Akt pathways. In the brown module, genes were enriched in ion transmembrane transport and exocytosis. Taken together, genes in the red modules were found to be most significantly correlated with GBM occurrence and progression.

In summary, using a series of bioinformatics analyses, this study illustrated hub genes and pathways that may be involved in progression

of GBM, based on DEGs screened from large GBM samples. Nevertheless, further molecular biological experiments are necessary to confirm the function of candidate biomarkers in GBM.

Acknowledgements

The excellent technical assistance of Yongwen Luo is gratefully acknowledged.

Disclosure of conflict of interest

None.

Address correspondence to: Dr. Xiang Peng, Department of Neurosurgery, Pu'ai Hospital, Tongji Medical College, Huazhong University of Science and Technology, Wuhan, China. Tel: +86-17740522459; E-mail: pengxiangdoc@163.com

References

[1] Ostrom QT, Gittleman H, Xu J, Kromer C, Wolinsky Y, Kruchko C and Barnholtz-Sloan JS. CBTRUS statistical report: primary brain and other central nervous system tumors diagnosed in the United States in 2009-2013. Neuro Oncol 2016; 18: v1-v75.

[2] Hellmark T and Segelmark M. Diagnosis and classification of Goodpasture's disease (anti-GBM). J Autoimmun 2014; 48-49: 108-112.

[3] Ostrom QT, Bauchet L, Davis FG, Deltour I, Fisher JL, Langer CE, Pekmezci M, Schwartzbaum JA, Turner MC, Walsh KM, Wrensch MR and Barnholtz-Sloan JS. The epidemiology of glioma in adults: a "state of the science" review. Neuro Oncol 2014; 16: 896-913.

[4] Wheeler CJ, Black KL, Liu G, Mazer M, Zhang XX, Pepkowitz S, Goldfinger D, Ng H, Irvin D and Yu JS. Vaccination elicits correlated immune and clinical responses in glioblastoma multiforme patients. Cancer Res 2008; 68: 5955-5964.

[5] Wang A and Zhang G. Differential gene expression analysis in glioblastoma cells and normal human brain cells based on GEO database. Oncol Lett 2017; 14: 6040-6044.

[6] Bo L, Wei B, Li C, Wang Z, Gao Z and Miao Z. Identification of potential key genes associated with glioblastoma based on the gene expression profile. Oncol Lett 2017; 14: 2045-2052.

[7] Langfelder P and Horvath S. WGCNA: an R package for weighted correlation network analysis. BMC Bioinformatics 2008; 9: 559.

[8] He Z, Sun M, Ke Y, Lin R, Xiao Y, Zhou S, Zhao H, Wang Y, Zhou F and Zhou Y. Identifying biomarkers of papillary renal cell carcinoma associated with pathological stage by weighted gene co-expression network analysis. Oncotarget 2017; 8: 27904-27914.

[9] Chen P, Wang F, Feng J, Zhou R, Chang Y, Liu J and Zhao Q. Co-expression network analysis identified six hub genes in association with metastasis risk and prognosis in hepatocellular carcinoma. Oncotarget 2017; 8: 48948-48958.

[10] Murat A, Migliavacca E, Gorlia T, Lambiv WL, Shay T, Hamou MF, de Tribolet N, Regli L, Wick W, Kouwenhoven MC, Hainfellner JA, Heppner FL, Dietrich PY, Zimmer Y, Cairncross JG, Janzer RC, Domany E, Delorenzi M, Stupp R and Hegi ME. Stem cell-related "self-renewal" signature and high epidermal growth factor receptor expression associated with resistance to concomitant chemoradiotherapy in glioblastoma. J Clin Oncol 2008; 26: 3015-3024.

[11] Griesinger AM, Birks DK, Donson AM, Amani V, Hoffman LM, Waziri A, Wang M, Handler MH and Foreman NK. Characterization of distinct immunophenotypes across pediatric brain tumor types. J Immunol 2013; 191: 4880-4888.

[12] Reifenberger G, Weber RG, Riehmer V, Kaulich K, Willscher E, Wirth H, Gietzelt J, Hentschel B, Westphal M, Simon M, Schackert G, Schramm J, Matschke J, Sabel MC, Gramatzki D, Felsberg J, Hartmann C, Steinbach JP, Schlegel U, Wick W, Radlwimmer B, Pietsch T, Tonn JC, von Deimling A, Binder H, Weller M and Loeffler M. Molecular characterization of long-term survivors of glioblastoma using genome- and transcriptome-wide profiling. Int J Cancer 2014; 135: 1822-1831.

[13] Gautier L, Cope L, Bolstad BM and Irizarry RA. Affy--analysis of Affymetrix GeneChip data at the probe level. Bioinformatics 2004; 20: 307-315.

[14] Leek JT and Storey JD. Capturing heterogeneity in gene expression studies by surrogate variable analysis. PLoS Genet 2007; 3: 1724-1735.

[15] Ritchie ME, Phipson B, Wu D, Hu Y, Law CW, Shi W and Smyth GK. limma powers differential expression analyses for RNA-sequencing and microarray studies. Nucleic Acids Res 2015; 43: e47.

[16] Szklarczyk D, Franceschini A, Wyder S, Forslund K, Heller D, Huerta-Cepas J, Simonovic M, Roth A, Santos A, Tsafou KP, Kuhn M, Bork P, Jensen LJ and von Mering C. STRING v10: protein-protein interaction networks, integrated over the tree of life. Nucleic Acids Res 2015; 43: D447-452.

[17] Shannon P, Markiel A, Ozier O, Baliga NS, Wang JT, Ramage D, Amin N, Schwikowski B and Ideker T. Cytoscape: a software environ-

ment for integrated models of biomolecular interaction networks. Genome Res 2003; 13: 2498-2504.
[18] Bader GD and Hogue CW. An automated method for finding molecular complexes in large protein interaction networks. BMC Bioinformatics 2003; 4: 2.
[19] Dennis G Jr, Sherman BT, Hosack DA, Yang J, Gao W, Lane HC and Lempicki RA. DAVID: database for annotation, visualization, and integrated discovery. Genome Biol 2003; 4: P3.
[20] Langfelder P, Luo R, Oldham MC and Horvath S. Is my network module preserved and reproducible? PLoS Comput Biol 2011; 7: e1001057.
[21] Tang Z, Li C, Kang B, Gao G, Li C and Zhang Z. GEPIA: a web server for cancer and normal gene expression profiling and interactive analyses. Nucleic Acids Res 2017; 45: W98-W102.
[22] Lin M, Zhang X, Jia B and Guan S. Suppression of glioblastoma growth and angiogenesis through molecular targeting of methionine aminopeptidase-2. J Neurooncol 2018; 136: 243-254.
[23] Athanasios A, Charalampos V, Vasileios T and Ashraf GM. Protein-protein interaction (PPI) network: recent advances in drug discovery. Curr Drug Metab 2017; 18: 5-10.
[24] Labbe DP, Sweeney CJ, Brown M, Galbo P, Rosario S, Wadosky KM, Ku SY, Sjostrom M, Alshalalfa M, Erho N, Davicioni E, Karnes RJ, Schaeffer EM, Jenkins RB, Den RB, Ross AE, Bowden M, Huang Y, Gray KP, Feng FY, Spratt DE, Goodrich DW, Eng KH and Ellis L. TOP2A and EZH2 provide early detection of an aggressive prostate cancer subgroup. Clin Cancer Res 2017; 23: 7072-7083.
[25] Okura H, Golbourn BJ, Shahzad U, Agnihotri S, Sabha N, Krieger JR, Figueiredo CA, Chalil A, Landon-Brace N, Riemenschneider A, Arai H, Smith CA, Xu S, Kaluz S, Marcus AI, Van Meir EG and Rutka JT. A role for activated Cdc42 in glioblastoma multiforme invasion. Oncotarget 2016; 7: 56958-56975.
[26] Li QQ, Hsu I, Sanford T, Railkar R, Balaji N, Sourbier C, Vocke C, Balaji KC and Agarwal PK. Protein kinase D inhibitor CRT0066101 suppresses bladder cancer growth in vitro and xenografts via blockade of the cell cycle at G2/M. Cell Mol Life Sci 2018; 75: 939-963.
[27] Tsavaris N, Lazaris A, Kosmas C, Gouveris P, Kavantzas N, Kopterides P, Papathomas T, Agrogiannis G, Zorzos H, Kyriakou V and Patsouris E. Topoisomerase I and IIalpha protein expression in primary colorectal cancer and recurrences following 5-fluorouracil-based adjuvant chemotherapy. Cancer Chemother Pharmacol 2009; 64: 391-398.
[28] Humphrey PA, Wong AJ, Vogelstein B, Friedman HS, Werner MH, Bigner DD and Bigner SH. Amplification and expression of the epidermal growth factor receptor gene in human glioma xenografts. Cancer Res 1988; 48: 2231-2238.
[29] Eskilsson E, Rosland GV, Solecki G, Wang Q, Harter PN, Graziani G, Verhaak RG, Winkler F, Bjerkvig R and Miletic H. EGFR heterogeneity and implications for therapeutic intervention in glioblastoma. Neuro Oncol 2018; 20: 743-752.
[30] Zhou YH, Chen Y, Hu Y, Yu L, Tran K, Giedzinski E, Ru N, Gau A, Pan F, Qiao J, Atkin N, Ly KC, Lee N, Siegel ER, Linskey ME, Wang P and Limoli C. The role of EGFR double minutes in modulating the response of malignant gliomas to radiotherapy. Oncotarget 2017; 8: 80853-80868.
[31] Fourest-Lieuvin A, Peris L, Gache V, Garcia-Saez I, Juillan-Binard C, Lantez V and Job D. Microtubule regulation in mitosis: tubulin phosphorylation by the cyclin-dependent kinase Cdk1. Mol Biol Cell 2006; 17: 1041-1050.
[32] Song Z, Pan Y, Ling G, Wang S, Huang M, Jiang X and Ke Y. Escape of U251 glioma cells from temozolomide-induced senescence was modulated by CDK1/survivin signaling. Am J Transl Res 2017; 9: 2163-2180.